

Parametric Design and Optimization of Multi-Rotor Aerial Vehicles

C. Ampatis and E. Papadopoulos

Abstract This work addresses the problem of optimal selection of propulsion components for a multi-rotor aerial vehicle (MRAV), for a given payload, payload capacity, number of rotors, and flight duration. Considering that the main components include motors, propellers, electronic speed controllers (ESC), and batteries, a steady state model is developed for each component using simplified analysis. Based on technical specifications of commercially available batteries, motors and ESCs, component functional parameters identified earlier were expressed as a function of component size, in terms of an equivalent length. Propeller models were developed using available experimental data. Airframe dimensions and total weight were expressed as a function of propeller diameter, number of rotors, and maximum thrust. Using Matlab's "fmincon" function, a program was developed which calculates the optimal design vector using the total energy consumption and vehicle diameter as objective function. Using the developed program, the influence of the payload and of the number of rotors on the design vector and the MRAV size was studied. The results obtained by the program were compared to existing commercial MRAVs.

Keywords Multi-rotor aerial vehicle (MRAV) design • Parametric design • Constrained optimization • Energy and size minimization

C. Ampatis • E. Papadopoulos (✉)
Department of Mechanical Engineering, National Technical University of Athens, Greece
e-mail: christos.ampatis@gmail.com; egpapado@central.ntua.gr

Introduction

22

Recently, Multi-Rotor Aerial Vehicles (MRAV) are encountered in an increasing 23 number of military and civilian applications. A particular advantage an MRAV 24 has over other aerial vehicles is its unique ability for vertical stationary flight 25 (VTOL). Micro and mini MRAVs with payload capabilities of up to 100 g and 26 2 kg respectively [1] offer major advantages when used for aerial surveillance and 27 inspection in complex and dangerous indoor and outdoor environments. In addition, 28 improvements and availability in cost-effective batteries and other technologies are 29 rapidly increasing the scope for commercial opportunities. 30

In most MRAV configurations, rotors are in the same plane and symmetrically 31 fixed on the airframe. The number of rotors is always even in order to balance 32 the torque produced by the rotors. An exception is the trirotor, where one rotor 33 is placed on a tilting mechanism in order to balance the excess torque. Additional 34 configurations include MRAVs with multiple pairs of coaxial-counter rotating 35 rotors. However, researchers push the limits by studying different configurations 36 where the rotors are not in the same plane but placed arbitrarily in 3D space [2], or 37 even having the ability of thrust vectoring [3, 4]. 38

In any configuration, an MRAV design consists of basic components, such as 39 batteries, electric motors, and propellers, which constitute the vehicle propulsion 40 system. One of the most critical stages in MRAV design is the proper motor- 41 propeller matching. The electric motor market offers a large range of motors 42 for almost any application, thus an MRAV designer does not need to design the 43 motor. Propellers used for MRAV applications are taken from the remote controlled 44 (RC) aircraft market, therefore they are designed for RC aircrafts. However, an 45 MRAV hovers for a great percent of the total flight time, therefore needs propellers 46 designed for maximum hover efficiency. Recently, the MRAV industry produced 47 such propellers but in a limited range. Recent studies resulted in optimized designs 48 of micro and mini rotorcraft vehicle propellers that are easy to manufacture, such as 49 curved plate plastic propellers, [5, 6]. 50

Apart from optimizing each MRAV component separately, an MRAV designer 51 would benefit from an automated design method that would take into account all 52 design requirements to yield an optimized combination of commercially available 53 components. Although studies on automated design methods exist [7, 8], no 54 method exists that takes into account both the propulsion system modeling and the 55 functional parameters of existing components. 56

In this paper, we propose an MRAV design method, which selects the optimum 57 propulsion system components. Given the MRAV design requirements such as 58 payload, payload capacity, number of rotors, and flight duration, a Matlab program 59 calculates the propulsion system components and MRAV size which leads to an 60 energy-efficient design, or to a design with the smallest size. To achieve this we use 61 simplified models for each component, and expressions of component functional 62 parameters as a function of component size, using their commercially available 63 technical specifications. 64

Component and System Modeling

65

The components to be modeled include the electric motors, the electronic speed controller, batteries, propellers, and the airframe. Combining the simplified models will lead to a system model for the MRAV steady state operation.

66

67

68

Electric Motor Model

69

The electric motors used in MRAV applications are outrunner Brushless Direct Current (BLDC) ones. This is due to their high efficiency and high torque constant (K_T), which allows direct propeller coupling (no gearbox). Although a BLDC motor is a synchronous 3-phase permanent magnet motor, it can be modeled as a permanent magnet DC motor. This leads to a classic three-constant model, see Fig. 1.

70

In Fig. 1, V_k is the supply voltage (V), i_a is the current through the motor coils (A), e_a is the back-electromotive force (EMF) (V), R_a is the armature resistance (Ω), M is the torque produced by the motor (Nm), and ω is its shaft angular velocity (rad/s). The equations describing the motor are:

75

$$V_k = e_a + i_a R_a \quad (1)$$

$$e_a = K_e \omega = K_T \omega = N / K_V \quad (2)$$

where K_e is the motor back EMF constant (Vs/rad), K_T is the motor torque constant (Nm/A), N is the motor rpm, and K_V is motor speed constant (rpm/V). The K_T is related to K_V by:

80

81

82

$$K_e = K_T = \frac{30}{\pi} \frac{1}{K_V} \quad (3)$$

The total torque produced by the motor is:

83

$$M = K_T i_a \quad (4)$$

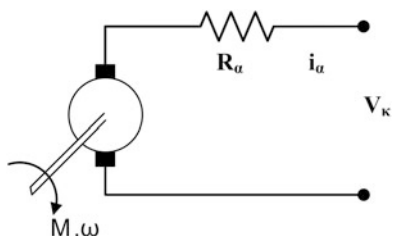


Fig. 1 Electric motor model

The output torque is:

84

$$M_{\text{mot}} = K_T (i_a - i_0) \quad (5)$$

where i_0 is the no-load current. The motor input power is:

85

$$P_{\text{in}} = V_k i_a \quad (6)$$

the motor output power is:

86

$$\begin{aligned} P_{\text{mot}} &= M_{\text{mot}} \omega = K_T (i_a - i_0) \omega = e_a (i_a - i_0) \\ &= (V_k - i_a R_a) (i_a - i_0) \end{aligned} \quad (7)$$

and the motor speed in rpm is:

87

$$N = (V_k - i_a R_a) K_V \quad (8)$$

Given the parameters K_T , R_a , and i_0 we can calculate the performance of the motor. 88

Electronic Speed Controller Model

89

Electronic speed controllers regulate motor speed within a range depending on the 90 load and battery voltage. The important quantity here is the ESC power losses, 91 caused by its power MOSFETs. The major parameters that affect ESC power losses 92 are the transistor drain-to-source “ON” state resistance $R_{\text{DS(ON)}}$, transistor charac- 93 teristics on transient operation, and the frequency switching the transistor “ON” and 94 “OFF.” Power losses at full throttle, when transistors are fully “ON,” depend only 95 on $R_{\text{DS(ON)}}$, while at partially opened throttle, when the transistors switch between 96 “ON” and “OFF,” additional power losses occur. 97

The range of $R_{\text{DS(ON)}}$ lies between 3 and 15 mΩ and its value is proportional 98 to transistor size. Considering that ESC power losses are a small portion of input 99 power, and the fact that ESC manufacturers do not include in ESC documentation 100 the type of transistors used, we model the ESC as a constant value resistor of 101 $R_{\text{DS(ON)}} = 5 \text{ m}\Omega$. BLDC motor ESCs use three pairs of transistors to manage the 102 three phase current, so the total resistance of the ESC will be: 103

$$R_{\text{ESC}} = 3R_{\text{DS(ON)}} = 0.015\Omega \quad (9)$$

Another important quantity of ESC is the maximum current i_{ESC} they can handle. 104 This appears as a design constraint. 105

Battery Model

106

Due to their high energy density and discharge rate, MRAVs use Lithium Polymer 107 (LiPo) batteries. A LiPo pack consists of identical LiPo cells each with a nominal 108 voltage of 3.7 V. Parallel connection of battery packs raises the battery total capacity, 109 while keeping the nominal total voltage the same. Therefore, the nominal total 110 voltage of a LiPo battery is: 111

$$V_b = n_c 3.7 \quad (10)$$

where n_c is the number of cells connected in series in a battery pack. The battery has 112 an internal total resistance $R_{\text{bat,tot}}$. When connected to a load its output voltage is: 113

$$V_{b,\text{out}} = V_b - i R_{\text{bat,tot}} \quad (11)$$

where i is the load current. 114

Each cell has internal resistance R_{sc} , capacity C_{sc} , and maximum discharge rate 115 DR_c . The total battery capacity is: 116

$$C_{\text{tot}} = n_p C_{\text{sc}} \quad (12)$$

where n_p is the number of battery packs connected in parallel. Each cell's power is: 117

$$P_{\text{sc}} = 3.7 D R_c C_{\text{sc}} \quad (13)$$

Each cell's energy is: 118

$$E_{\text{sc}} = 3.7 C_{\text{sc}} \quad (14)$$

A battery's total power is: 119

$$P_{\text{bat,tot}} = P_{\text{sc}} n_c n_p \quad (15)$$

while its total energy is: 120

$$E_{\text{bat,tot}} = E_{\text{sc}} n_c n_p \quad (16)$$

To calculate $R_{\text{bat,tot}}$ we apply Kirchoff's law to a battery consisted of n_p identical 121 packs connected in parallel, each of which consists of n_c identical cells connected 122 in series. Each battery pack has an internal resistance: 123

$$R_i = n_c R_{\text{sc}}, \quad i = 1, \dots, n_p \quad (17)$$

The battery total resistance is: 124

$$R_{\text{bat,tot}} = \prod_{j=1}^{n_p} R_j \left/ \sum_{i=1}^{n_p} \left(\frac{1}{R_i} \prod_{j=1}^{n_p} R_j \right) \right. = \frac{(n_c R_{\text{sc}})^{n_p}}{n_p (n_c R_{\text{sc}})^{n_p-1}} = \frac{n_c R_{\text{sc}}}{n_p} \quad (18)$$

Propeller Model

125

Propellers used on MRAVs are mostly the same propellers used in remote controlled (RC) airplanes. Propeller performance is described by its thrust T (N), power P (W), and torque M (Nm). To model performance in static conditions, we use manufacturer data such as propeller diameter D_p and its pitch p at 75 % of its radius. Performance quantities are then related to propeller speed, diameter, and pitch. This is achieved through a number of coefficients.

The thrust coefficient is given by:

$$C_T = T / \rho (N/60)^2 D^4 \quad (19)$$

where T is thrust (N), ρ is air density (kg/m^3), N is propeller speed (rpm), and D is the propeller diameter (m).

The power coefficient is given by:

$$C_P = P / \rho (N/60)^3 D^5 \quad (20)$$

where P is power (W).

The torque coefficient is given by:

$$C_M = M / \rho (N/60)^2 D^5 \quad (21)$$

where M is torque (Nm). Using the fundamental relation between power, torque, and speed we get:

$$C_M = C_P / 2\pi \quad (22)$$

These coefficients are next related to propeller diameter and pitch. Using the Blade Element Momentum Theory (BEMT) and a series of assumptions [9], we get the following equations for thrust and power coefficients:

$$C_T = \frac{\pi^3}{4} \frac{1}{2} \sigma C_{la} \left(\frac{\theta_{0.75}}{3} - \frac{1}{2} \sqrt{\frac{4}{\pi^3} \frac{C_T}{2}} \right) \quad (23)$$

$$C_P = \frac{2}{\pi^2} \frac{C_T^{3/2}}{\sqrt{2}} + \frac{1}{8} \sigma C_{d0} \quad (24)$$

where σ is propeller solidity, C_{la} is the slope of blade airfoil lift coefficient– incidence angle curve, $\theta_{0.75}$ is propeller pitch angle at 75 % of the propeller radius R , and C_{d0} is a blade's airfoil drag coefficient for zero lift.

To further simplify this model to a restricted propeller size range and geometry, we make the following assumptions. Considering that we refer to geometrically

scaled propellers, propeller solidity σ will be constant regardless of propeller size. 148
 Additionally, if the propeller size range is no more than one order of magnitude, 149
 then the Reynolds number does not change dramatically, so we can assume that the 150
 aerodynamic quantities $C_{l\alpha}$ and C_{d0} are constant. Consequently, thrust and power 151
 coefficients are only a function of propeller pitch angle $\theta_{0.75}$. From the definition of 152
 geometric pitch we get: 153
 153

$$p = 2\pi R \tan \theta \quad (25)$$

and therefore, the geometric pitch at $0.75R$ will be: 154

$$p_{0.75} = 2\pi \frac{3}{4} R \tan \theta_{0.75} = \pi \frac{3}{4} D_p \tan \theta_{0.75} \quad (26)$$

Solving Eq. (26) for $\theta_{0.75}$ we get: 155

$$\theta_{0.75} = \arctan (4/3\pi \cdot p_{0.75}/D_p) \quad (27)$$

Consequently, using Eqs. (23), (24), and (27) we can relate C_T and C_P to the ratio 156
 $p_{0.75}/D_p$ only. Normally, $\theta_{0.75}$ is in the range of 5–30, resulting a $p_{0.75}/D_p$ range of 157
 0.2–1.35. In this region the function $C_T(p_{0.75}/D_p)$ is linear and this can be shown 158
 through a numerical solution. Additionally, by observing Eq. (24) we see that C_P is 159
 proportional to $C_T^{3/2}$, therefore it is proportional to $(p_{0.75}/D_p)^{3/2}$, and this can be 160
 also shown through a numerical solution in the $p_{0.75}/D_p$ range. 161

Consequently, we get the simplified expressions for thrust and power coefficients: 162

$$C_T = k_1 (p/D_p) + k_2 \quad (28)$$

$$C_P = k_3 (p/D_p)^{3/2} + k_4 \quad (29)$$

where constants k_1 to k_4 can be calculated using experimental data of geometrically 163
 scaled propellers. 164

Note that to obtain energy efficient propellers at hover, the ratio C_T/C_P must 165
 be as high as possible. Solving Eqs. (23) and (24) or (28) and (29), we see that this 166
 occurs when the ratio p/D_p is as low as possible, i.e., for a given propeller diameter 167
 the lowest pitch yields more efficient propellers. 168

System Model

169

The system model results from the combination of the propulsion system model and 170
 the equilibrium of forces acting on the vehicle. The propulsion system consists of 171
 the battery and n_{mot} triples of ESC, and of the motors and propellers connected in 172
 parallel, as shown in Fig. 2. 173

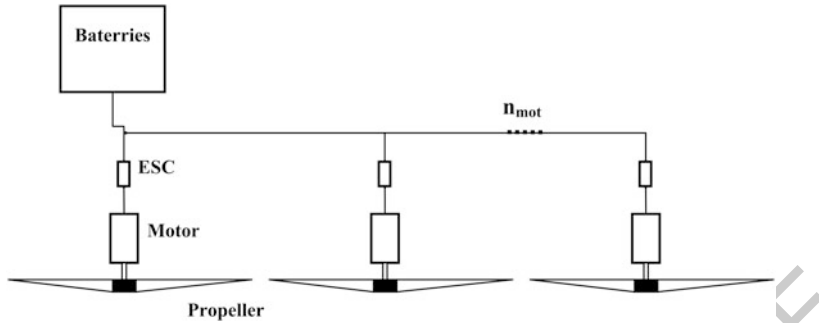


Fig. 2 Propulsion system

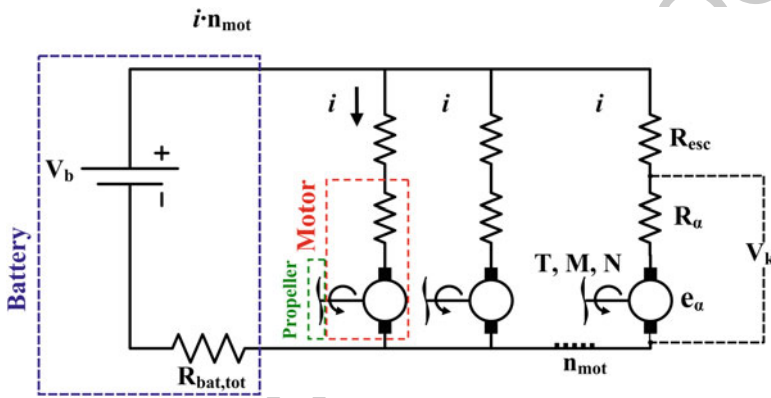


Fig. 3 Propulsion system physical model

The physical model of the propulsion system shown in Fig. 3 combines each component model and outputs the total thrust produced by the n_{mot} rotors. Assuming that all the rotors have the same speed, the current drawn will be the same for each motor.

Applying Kirchoff's law to the circuit of Fig. 3 we get:

$$V_k + i R_{\text{ESC}} = V_b - n_{\text{mot}} i R_{\text{bat,tot}} \quad (30)$$

$$e_a = V_b - i (R_a + R_{\text{ESC}} + n_{\text{mot}} R_{\text{bat,tot}}) \quad (31)$$

The rotor speed is given by:

$$N = [V_b - i (R_a + R_{\text{ESC}} + n_{\text{mot}} R_{\text{bat,tot}})] K_V \quad (32)$$

The above equation is valid only at full throttle, when the ESC transistors are fully on; otherwise, at partially open throttle, the ESC output voltage is less than the maximum, thus the motor voltage will be less than V_k .

Equation (32) shows that the motor equivalent resistance is:

183

$$R_{\text{tot}} = R_a + R_{\text{ESC}} + n_{\text{mot}} R_{\text{bat,tot}} \quad (33)$$

In this paper we examine the case where the vehicle during a total flight time t_{tot} has two operational modes. (a) A *maximum thrust mode* for a percentage ATP of the total flight time t_{tot} , in which motors are at full throttle state producing the maximum static thrust, and (b) a *hover mode*, in which the vehicle hovers for the rest of the flight time. At maximum thrust, the vehicle has the ability to accelerate with an instantaneously maximum acceleration, therefore it has the ability to lift its total weight f_w times.

(a) Maximum thrust mode: The rotor speed is:

191

$$N_{\text{acc}} = [V_b - i_{\text{acc}} R_{\text{tot}}] K_V \quad (34)$$

which is equivalent to the following:

192

$$N_{\text{acc}} = [V_{k,\text{acc}} - i_{\text{acc}} R_a] K_V \quad (35)$$

where $V_{k,\text{acc}}$ is the motor supply voltage equal to the maximum ESC output voltage.

193

194

A balance of forces, with a the acceleration, yields:

195

$$\begin{aligned} \Sigma F = m_{\text{tot}} a &\Rightarrow n_{\text{mot}} T_{\text{acc}} - m_{\text{tot}} g = m_{\text{tot}} a = (f_w - 1) m_{\text{tot}} g \\ &\Rightarrow n_{\text{mot}} C_T \rho (N_{\text{acc}}/60)^2 D_p^4 = f_w m_{\text{tot}} g \end{aligned} \quad (36)$$

The maximum instantaneous linear acceleration will be:

196

$$a = (f_w - 1) g \quad (37)$$

The total mass of the vehicle is:

197

$$m_{\text{tot}} = m_{\text{bat,tot}} + (m_{\text{mot}} + m_p + m_{\text{ESC}}) n_{\text{mot}} + m_{\text{frm}} + m_{\text{pl}} \quad (38)$$

where $m_{\text{bat,tot}}$ is the battery total mass, m_{mot} is the motor mass, m_p is the propeller mass, m_{ESC} is the ESC mass, m_{frm} is the airframe mass, and m_{pl} is the payload mass.

198

199

200

The equation of motor-propeller power is:

201

$$P_m = P \Rightarrow \{V_b - i_{\text{acc}} R_{\text{tot}}\} (i_{\text{acc}} - i_0) = C_P \rho (N_{\text{acc}}/60)^3 D_p^5 \quad (39)$$

The motor-propeller torque balance yields:

202

$$M_m = M \Rightarrow K_T (i_{\text{acc}} - i_0) = C_P \rho (N_{\text{acc}}/60)^2 D_p^5 / 2\pi \quad (40)$$

The system input power is:

203

$$P_{\text{IN,acc}} = V_b i_{\text{acc}} n_{\text{mot}} \quad (41)$$

while the system energy consumption is:

204

$$E_{\text{IN,acc}} = P_{\text{IN}} t_{\text{tot}} ATP \quad (42)$$

(b) Hover mode: In this mode, the motor speed is:

205

$$N_{\text{hov}} = [V_{k,\text{hov}} - i_{\text{hov}} R_a] K_V \quad (43)$$

where $V_{k,\text{hov}}$ is ESC output voltage that satisfies $V_{k,\text{hov}} < V_{k,\text{acc}}$.

206

The balance of forces yields:

207

$$\begin{aligned} \sum F = 0 \Rightarrow n_{\text{mot}} T_{\text{hov}} &= m_{\text{tot}} g \Rightarrow \\ n_{\text{mot}} C_T \rho (N_{\text{hov}}/60)^2 D_p^4 &= m_{\text{tot}} g \end{aligned} \quad (44)$$

The equation of motor-propeller power is:

208

$$P_m = P \Rightarrow$$

209

$$\{V_{k,\text{hov}} - i_{\text{hov}} R_a\} (i_{\text{hov}} - i_0) = C_P \rho (N_{\text{hov}}/60)^3 D_p^5 \quad (45)$$

210

while the motor-propeller torque balance gives:

211

$$M_m = M \Rightarrow$$

212

$$K_T (i_{\text{hov}} - i_0) = (1/2\pi) C_P \rho (N_{\text{hov}}/60)^2 D_p^5 \quad (46)$$

213

The system input power is:

214

$$P_{\text{IN,hov}} = V_b i_{\text{hov}} n_{\text{mot}} \quad (47)$$

and the system energy consumption is:

215

$$E_{\text{IN,hov}} = P_{\text{IN,hov}} t_{\text{tot}} (1 - ATP) \quad (48)$$

Battery total power is constrained by:

216

$$P_{\text{IN,acc}} \leq P_{\text{bat,tot}} \quad (49)$$

while the battery total energy is given by:

217

$$E_{\text{IN,hov}} + E_{\text{IN,acc}} = E_{\text{tot}} = E_{\text{bat,tot}} \quad (50)$$

Parameterization

218

The system equations given in the previous section depend on the functional parameters, which define components performance. Here, these parameters are expressed as a function of component length. This length is taken as the cubic root of a component's volume (cubic length) and is referred to as the *equivalent length*. We do the same with propellers using available experimental measurements. Furthermore, we develop equations that correlate airframe size as a function of propeller diameter, number of rotors, and maximum thrust.

Electric Motor

226

The electric motors we chose for parameterization are the outrunner BLDC motors from AXI manufacturer. The choice is based on the technical specifications available and on the reliability and performance of these motors.

Here, the equivalent length of each motor is related to the outer dimensions of the motor and not to its stator dimensions. The parameters we want to relate to the equivalent length are the motor armature resistance R_a , torque constant K_T , no load current i_0 , and motor mass m_{mot} . Additionally, motor maximum sustained current (or current capacity) i_{max} and motor maximum speed $N_{m,\text{max}}$ are parameters that limit motor performance and must be related to equivalent length.

Consequently, we need to develop five equations as functions of equivalent length. After investigation of various correlations of these parameters to the equivalent length, we concluded the following functions due to their optimal fit to manufacturer data. Below, R^2 refers to coefficient of determination, and l_{mot} to motor equivalent length (m).

$$K_T / R_a = 2.6533 \cdot 10^4 l_{\text{mot}}^{3.6032}, R^2 = 0.902 \quad (51)$$

$$K_T^2 / R_a = 1.7548 \cdot 10^5 l_{\text{mot}}^{5.4833}, R^2 = 0.94 \quad (52)$$

$$M_0 = K_T i_0 = 5.7721 \cdot 10^2 l_{\text{mot}}^{3.1888}, R^2 = 0.908 \quad (53)$$

$$M_{\text{max}} = K_T (i_{\text{max}} - i_0) = 4.5004 \cdot 10^5 l_{\text{mot}}^{4.2222}, R^2 = 0.96 \quad (54)$$

$$N_{m,\text{max}} = (n_{c,\text{max}} 3.7 - i_0 R_a) K_V \Rightarrow$$

$$N_{m,\text{max}} = 25604 e^{-17.687 l_{\text{mot}}}, R^2 = 0.35 \quad (55)$$

where $n_{c,\text{max}}$ is the maximum number of battery cells in series connection that is proposed by manufacturer.

241

242

To relate motor mass to motor equivalent length, we calculated the mean motor 243
density ρ_{mot} : 244

$$\rho_{\text{mot}} = 2942 \text{ kg/m}^3 \quad (56)$$

Using (56), the motor mass is: 245

$$m_{\text{mot}} = \rho_{\text{mot}} l_{\text{mot}}^3 \quad (57)$$

Electronic Speed Controller

246

We chose to parameterize ESCs from JETI due to the availability of technical 247
specifications and their performance. Although the ESC is modeled as a constant 248
resistance, additional parameters are needed that relate its operational limit and mass 249
properties to its equivalent length l_{ESC} (m). These parameters are the ESC maximum 250
sustained current i_{ESC} and ESC mean density ρ_{ESC} . 251

Using ESC technical specifications, correlations of maximum sustained current 252
 i_{ESC} and ESC equivalent length l_{ESC} are obtained as: 253

$$i_{\text{ESC}} = 8.4545 \cdot 10^6 l_{\text{ESC}}^{3.2451}, R^2 = 0.88 \quad (58)$$

The mean ESC density calculated as: 254

$$\rho_{\text{ESC}} = 2580 \text{ kg/m}^3 \quad (59)$$

yielding the ESC mass as: 255

$$m_{\text{ESC}} = \rho_{\text{ESC}} l_{\text{ESC}}^3 \quad (60)$$

Battery

256

We chose to parameterize batteries from Kokam for the same reasons as before. The 257
parameters to be related to battery total equivalent length l_{bat} include total power 258
 $P_{\text{bat,tot}}$, total energy $E_{\text{bat,tot}}$, total resistance $R_{\text{bat,tot}}$, and mass m_{bat} . 259

Battery technical specifications concern single battery cells of 3.7 V nominal 260
voltage. However, we need information for any combination of parallel and series 261
connected cells. We assume that n_p cells connected in parallel result in a larger 262
single cell with volume B_{vol} , power P_{bat} , energy E_{bat} , and internal resistance R_{bat} . 263

Assuming that the battery consists of $n_p n_c$ identical cells of volume $B_{\text{vol,sc}}$ each, 264
then an equivalent battery will consist of n_c equivalent cells each of which has 265
volume: 266

$$B_{\text{vol}} = n_p B_{\text{vol,sc}} \quad (61)$$

Therefore, each equivalent cell volume will be:

267

$$B_{\text{vol}} = l_{\text{bat}}^3 / n_c \quad (62)$$

Applying curve fitting to manufacturer data, the following equation for single cell internal resistance was obtained:

268

269

$$R_{\text{sc}} = 2.84668 \cdot 10^{-7} B_{\text{vol,sc}}^{-0.951154} \quad (63)$$

Correspondingly, the equivalent cell internal resistance is:

270

$$R_{\text{bat}} = 2.84668 \cdot 10^{-7} B_{\text{vol}}^{-0.951154}, R^2 = 0.95 \quad (64)$$

Using (18), (63), and (64), the battery total resistance is:

271

$$R_{\text{bat,tot}} = n_c R_{\text{sc}} / n_p = n_c 2.84668 \cdot 10^{-7} (B_{\text{vol}} / n_p)^{-0.951154} / n_p \Rightarrow \quad (65)$$

272

$$R_{\text{bat,tot}} = n_c R_{\text{bat}} n_p^{-(1-0.951154)} \approx n_c R_{\text{bat}} n_p^{-0.05} \quad (65)$$

273

However, n_p will never be large; therefore using the approximation $n_p^{0.05}$, battery total resistance will be:

274

275

$$R_{\text{bat,tot}} = n_c R_{\text{bat}} \quad (66)$$

Applying curve fitting to manufacturer data, we observe that cell energy and power are proportional to its volume. Therefore, using the mean value of the ratios cell energy to cell volume and cell power to cell volume yield:

276

277

278

$$P_{\text{bat}} = 7.0899 \cdot 10^6 B_{\text{vol}} \quad (67)$$

$$E_{\text{bat}} = 9.0833 \cdot 10^8 B_{\text{vol}} \quad (68)$$

Using (67) and (68), the battery total power and energy are:

279

$$P_{\text{bat,tot}} = n_c P_{\text{bat}} \quad (69)$$

$$E_{\text{bat,tot}} = n_c E_{\text{bat}} \quad (70)$$

The mean battery cell density is calculated as:

280

$$\rho_{\text{bat}} = 1907.8 \text{ kg/m}^3 \quad (71)$$

Yielding the battery total mass:

281

$$m_{\text{bat}} = \rho_{\text{bat}} B_{\text{vol}} n_c \quad (72)$$

Propeller

282

The propellers we chose to parameterize are taken from APC. The parameters to be related to propeller diameter D_p and geometric pitch p are the thrust and power coefficient, C_T and C_P respectively. 283
284
285

Previously, it was shown through Eqs. (28) and (29) that for zero flight velocity, C_T and C_P are functions of the ratio p/D_p . The constants k_1 through k_4 in these equations depend on propeller design and the Reynolds number. Here, we are interested in propellers with diameter of 80–500 mm, therefore we use experimental data for these dimensions, so as to satisfy Reynolds number. 286
287
288
289
290

Experiments on commercially available propellers used in remote controlled aircrafts were conducted at the University of Illinois, Urbana-Champaign (UIUC) in a wind tunnel [10]. Here, data regarding SPORT type APC propellers are used. From the C_T and C_P measurements for these propellers, those that refer to static conditions are used here. We observed that C_T and C_P are not affected much by propeller speed; therefore we calculated mean values of C_T and C_P for various speeds. These measurements concern propeller diameter of 7 in to 14 in. Finally, the C_T and C_P were correlated to the ratio p/D_p , obtaining the following functions: 291
292
293
294
295
296
297
298

$$C_T = 0.0266 (p/D_p) + 0.0793, R^2 = 0.31 \quad (73)$$

$$C_P = 0.0723 (p/D_p)^{3/2} + 0.0213, R^2 = 0.83 \quad (74)$$

The propeller mass is related to propeller diameter D_p as: 299

$$m_p = 0.97573 D_p^{2.5741}, R^2 = 0.98 \quad (75)$$

Number of Rotors

300

The number of MRAV rotors can be even or odd. MRAVs with odd number of rotors need an additional degree of freedom (tilting) for one rotor, so that it can vector its thrust and regulate excess torque produced by the rotors. This requires extra mechanisms (revolute joint) and an extra actuator to move the rotor. To take this into account, we assume that these extra mechanisms increase vehicle mass with a percentage $f_{M,odd}$ of the mass of one of the rods holding the motors. Additionally, actuator power increases total power with a percentage $f_{P,odd}$ of one motor power. Reasonable values for these coefficients are $f_{M,odd} = 0.5$ and $f_{P,odd} = 0.01$. 301
302
303
304
305
306
307
308

this figure will be printed in b/w

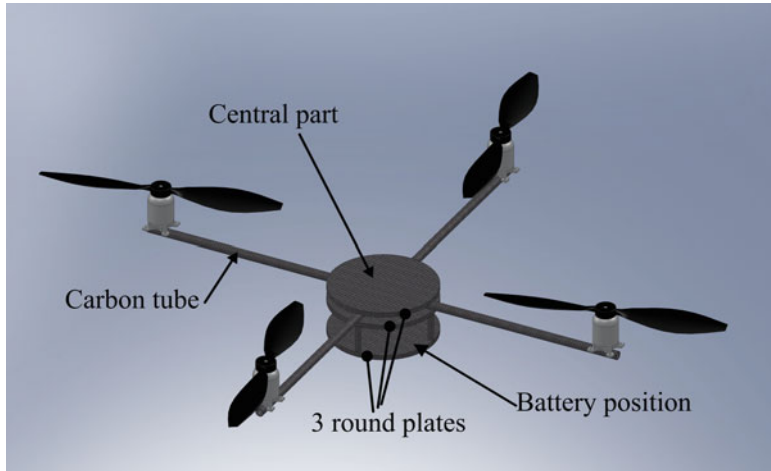


Fig. 4 MRAV airframe components

Airframe

309

Here, we are interested in the dimensions and mass properties of an MRAV airframe 310 of simple design, with respect to the number of rotors n_{mot} , propeller diameter D_p , 311 and airframe loading during flight. 312

A common rotor configuration is assumed. All rotors are in the same plane and 313 motors are equidistant lying on a circle with its center coincident to vehicle center. 314 The number of rotors is in the range of 3–8. 315

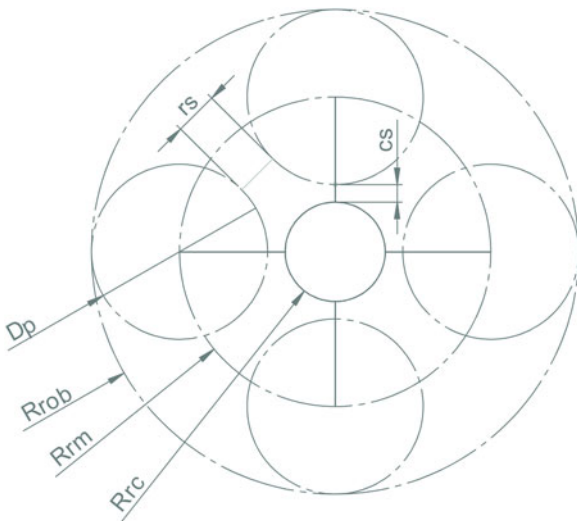
To approximate airframe mass its components and material must be assumed. 316 A reasonable design consists of n_{mot} rods to hold the motors, and a central part of 317 the three circular plates holding the rods and enclosing the battery and electronics. 318 Additionally, airframe material is carbon fiber due to its high strength to weight 319 ratio, and the accessories like screws and glue are a percentage $f_{\text{fr,ac}}$ of each rod 320 mass. An illustration of such an airframe is presented in Fig. 4. 321

Airframe dimensions are defined by propeller diameter and vehicle loading 322 during flight. On Fig. 5, airframe dimensions are shown. These include propeller 323 diameter D_p , rotor spacing r_s , central disk-rotor spacing c_s , center disk radius R_{rc} , 324 motor mounting position radius R_{rm} , and radius R_{rob} of the circle containing the 325 whole vehicle. Note that the radius R_{rm} is the same for each rod. For a given 326 propeller diameter, the dimensions r_s and c_s define the rest airframe dimensions. 327

The spacing r_s is important for a number of reasons. Primarily, if r_s is too 328 small, there is a danger of adjacent rotor collision during flight due to rod 329 elasticity. As was shown experimentally in [2] and [6], if r_s is too small, then 330 propeller performance deterioration due to adjacent propellers airflow interaction is

Fig. 5 Airframe dimensions

this figure will be printed in b/w



negligible. Furthermore, r_s cannot be too small because then the central disk will be 331 very small to accommodate the battery and control unit. Additionally, r_s cannot be 332 the same for all multi-rotors, i.e., a quadrotor must have a larger r_s than a hexarotor. 333 For the same reason, c_s must vary for different number of rotors. 334

Based on the design trials with respect to the above explanation, r_s and c_s were 335 expressed as a function of propeller radius R_p . Central disk thickness was expressed 336 as a reasonable function of R_{rc} . For the calculation of carbon tubes' diameter and 337 thickness, we developed equations that take into account material strength, tube 338 maximum deflection, and tube loading. These equations allow calculation of the 339 airframe mass. 340

Component Optimal Selection

341

In the previous sections, component performance was related to component equivalent length. Next, a method is developed for optimal selection of these lengths, 342 which are parameters of the design vector. This vector minimizes an objective 343 function, which is either the vehicle total energy, or the vehicle diameter D_{rob} . 344 345

Design Parameters

346

The design requirements are described by a number of parameters set by the 347 designer. These include the payload m_{pl} , the total flight time t_{tot} , the payload 348

capacity described by f_w indicating how many times the vehicle can lift its own weight, and the factor ATP which indicates the percentage of total flight time that the vehicle is at maximum thrust mode. 349
350
351

The design vector consists of the number of battery cells n_c in series, the 352 equivalent battery length l_{bat} , the equivalent motor length l_{mot} , the equivalent 353 ESC length l_{ESC} , the propeller diameter D_p , the ratio p/D_p , and the number of 354 rotors n_{mot} . 355

Design Vector Domain

356

The design vector domain results from the size limits of the components that were 357 parameterized earlier. Outside these regions the functions developed earlier may not 358 be valid. Hence, the design vector domain is: 359

$$0.01 \leq l_{\text{bat}} \leq 0.15 \text{ (m)} \quad (76a)$$

$$0.01 \leq l_{\text{mot}} \leq 0.08 \text{ (m)} \quad (76b)$$

$$0.005 \leq l_{\text{ESC}} \leq 0.05 \text{ (m)} \quad (76c)$$

$$0.05 \leq D_p \leq 0.5 \text{ (m)} \quad (76d)$$

$$0.2 \leq p/D_p \leq 1.5 \text{ (m)} \quad (76e)$$

$$1 \leq n_c \leq 10 \quad (76f)$$

Calculation Procedure

360

In every optimization step, the requirements vector $(m_{\text{pl}}, t_{\text{tot}}, f_w, ATP)$ is constant, 361 while the design vector $(n_c, l_{\text{bat}}, l_{\text{mot}}, l_{\text{ESC}}, D_p, p/D_p, n_{\text{mot}})$ changes until the mini- 362 363 mization of objective function is reached. 363

The calculation procedure follows the following sequence. The battery nominal 364 voltage V_b is calculated using Eq. (10). Using Eq. (36) we get: 364
365

$$N_{\text{acc}} = 60 \left(\frac{f_w m_{\text{tot}} g}{n_{\text{mot}} C_T \rho D_p^4} \right)^{1/2} \quad (77)$$

Using Eq. (40) we get: 366

$$i_{\text{acc}} = K_V C_P \rho \frac{N_{\text{acc}}^2}{60^3} D_p^5 + i_0 \quad (78)$$

Using Eq. (35) we get: 367

$$V_{k,\text{acc}} = \frac{N_{\text{acc}}}{K_V} + i_{\text{acc}} R_a \quad (79)$$

The motor maximum speed without load is:

368

$$N_{\max} = [V_b - i_0 R_{\text{tot}}] K_V \quad (80)$$

Using Eq. (41), the maximum total input power $P_{\text{IN,acc}}$ is calculated, while using Eq. (42) the total input energy at maximum thrust mode $E_{\text{IN,acc}}$ is calculated. Using Eq. (44) we get:

$$N_{\text{hov}} = 60 \left(\frac{m_{\text{tot}} g}{n_{\text{mot}} C_T \rho D_p^4} \right)^{1/2} \quad (81)$$

Using Eq. (46) we get:

372

$$i_{\text{hov}} = K_V C_P \rho \frac{N_{\text{hov}}^2}{60^3} D_p^5 + i_0 \quad (82)$$

Using Eq. (43) we get:

373

$$V_{k,\text{hov}} = \frac{N_{\text{hov}}}{K_V} + i_{\text{hov}} R_a \quad (83)$$

The total input energy at hover $E_{\text{IN,hov}}$ is obtained using Eq. (48), while using Eq. (50) the total input energy E_{tot} is found.

374

375

Constraints

376

The constraints result from the independent variable physical consistency. They are given as follows:

377

378

$$\begin{aligned} V_{\text{acc}} - V_b &\leq 0, N_{\text{acc}} - N_{\max} \leq 0, i_{\max} - i_{\text{ESC}} \leq 0 \\ i_{\text{acc}} - i_{\max} &\leq 0, i_{\text{hov}} - i_{\text{acc}} \leq 0, P_{\text{IN,acc}} - P_{\text{bat,tot}} \leq 0 \\ E_{\text{tot}} - E_{\text{bat,tot}} &\leq 0, -i_{\text{acc}} \leq 0, -i_{\max} \leq 0 \end{aligned} \quad (84)$$

Optimization Methodology

379

For the calculation procedure, a Matlab program was developed that employs the “fmincon” function (minimum of constrained nonlinear multivariable function) which uses one target deterministic constrained optimization method for nonlinear multivariable objective function.

380

381

382

383

Our target was to determine the most energy-efficient design or the smallest one. 384
Hence, the objectives were the minimization of battery energy $E_{\text{bat,tot}}$ or vehicle 385
diameter D_{rob} , respectively. 386

In order to check that “fmincon” will not be trapped in local minimums, we 387
also developed a program that scans the whole design vector domain, using nested 388
loops. We observed no differences between these methods after some test runs. 389
Consequently, “fmincon” calculates the total minimum for our objective functions. 390

Design Scenarios

391

Here we carry out some test runs in order to study the influence of payload and 392
number of rotors on the design vector and the MRAV size. In all design scenarios 393
below, the requirement parameters are set to: $t_{\text{tot}} = 15 \text{ min}$, $f_w = 2$, $ATP = 394$
 0.1 , $f_{\text{fr,ac}} = 0.15$, $f_{M,\text{odd}} = 0.5$, and $f_{P,\text{odd}} = 0.01$. Finally, we compare our 395
program results to commercially available MRAVs designs. 396

Study of Parameters Influence

397

Payload Influence

398

In this case payload changes from 0 to 1.5 kg, while the number of rotors is constant 399
and equal to 4. 400

In Fig. 6 the influence of payload on the design vector is shown. In general, we 401
observe that as the payload increases, component equivalent length increases due to 402
power increase. As expected, the ratio p/D_p is always constant and takes the lowest 403
value permitted, indicating that for a given propeller diameter, the propeller pitch 404
should always be the lowest. In addition, total energy minimization yields a more 405
efficient but a larger design than that obtained by minimizing vehicle size. However, 406
these differences are not large. 407

In Fig. 7, the influence of payload on total mass and on battery mass is illustrated. 408
We observe that the battery mass is always lower for the minimization of total 409
energy. However, vehicle total mass is not sensitive to the two objective functions. 410
This happens because a smaller vehicle has smaller and therefore lighter motors and 411
rotors. Additionally, observing the battery mass chart, we can say that battery mass 412
increases linearly with payload. For the quadrotor, we can say that we need 1.5 kg 413
batteries for 1 kg payload, and because the flight time is 15 min, then we can say 414
that for 1 kg payload we need 100 g batteries for every minute of flight. 415

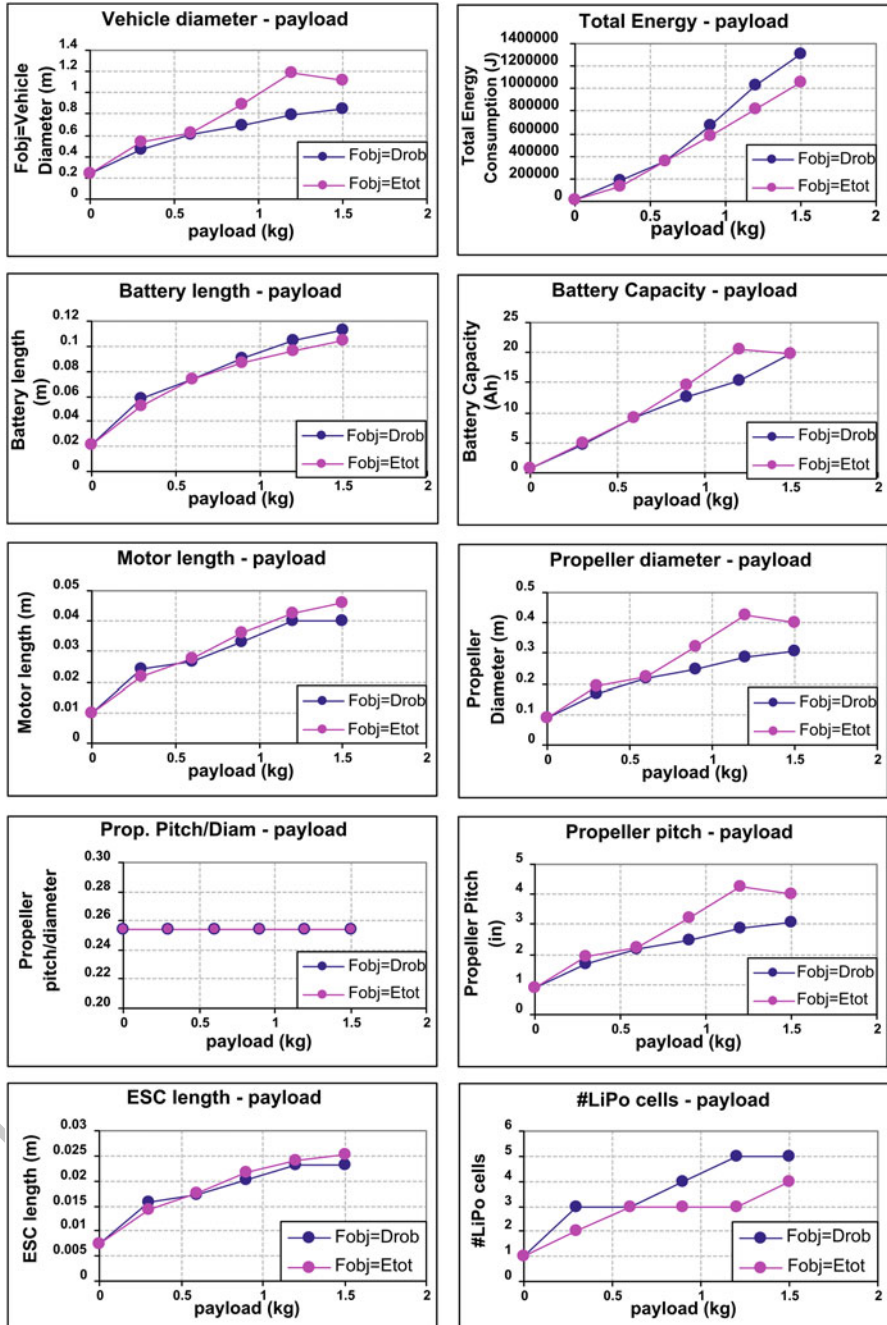


Fig. 6 Influence of payload on the design vector for the number of rotors equal to 4. Objective functions comparison

this figure will be printed in b/w

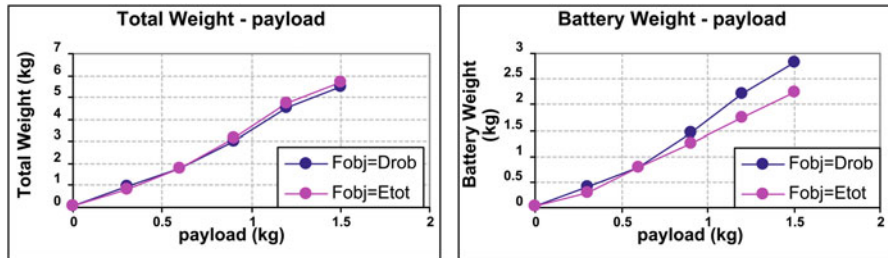


Fig. 7 Influence of payload on the total and battery mass for the number of rotors equal to 4. Objective functions comparison

Number of Rotors Influence

416

In this case, the number of rotors changes from 3 to 8, while the payload is constant 417 and equal to 1 kg. 418

In Fig. 8, the influence of rotors number on the design vector is presented. We 419 observe that for energy minimization, the best design has 8 rotors, but this is true 420 for a payload of 1 kg, see Fig. 9. Additionally, we observe the expected decrease in 421 components equivalent length when the number of rotors increases. 422

Test Cases

423

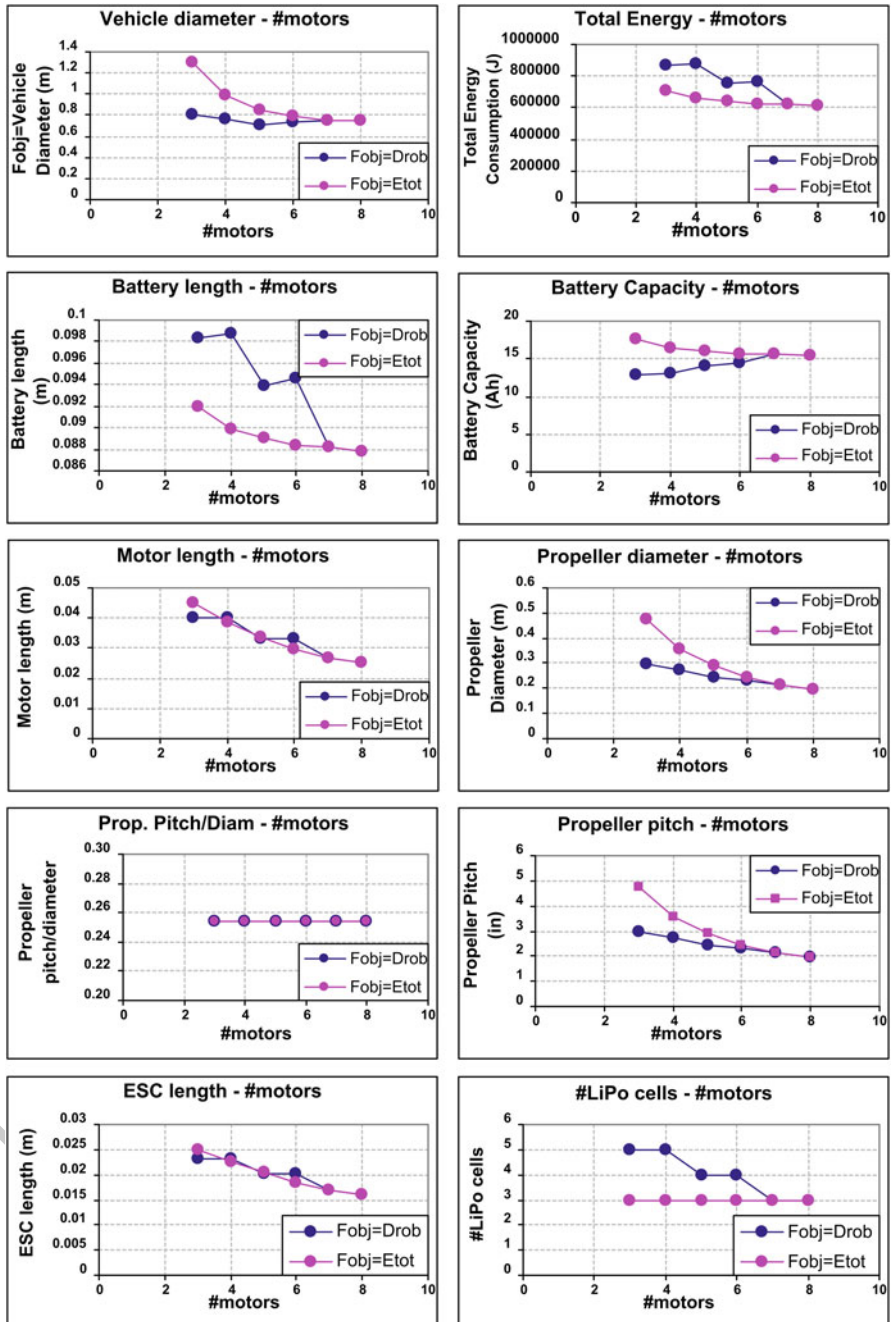
To determine whether the developed design methodology is valid and yields designs 424 close to reality, we compare program results to two existing commercial MRAVs. 425 The first is the quadrotor Walkera HM Hoten X Quadcopter, a small MRAV 426 designed for a payload less than 100 g. The other is the Octocopter X88-J2, a large 427 MRAV designed for aerial photography and for payloads up 1.5 kg, see Fig. 10. 428

Table 1 presents the quadrotor comparison, with data retrieved from [11]. The 429 payload includes the electronics and control unit. We observe that the program 430 yields results very close to reality. The difference lies on battery configuration 431 and mass. The existing vehicle uses two battery cells in series with total energy 432 23.7V1Ah=7.4Wh, while the optimized needs 13.7V1.611Ah=6Ah. Therefore, the 433 optimized vehicle seems to be more energy efficient. 434

In Table 2 an octocopter comparison is presented, with data taken from [12]. 435 Here we observe that the optimized vehicle is 8 % heavier but 25 % smaller. Also, 436 the optimized vehicle batteries have double capacity because there are two battery 437 cells in series. Thus, the optimized vehicle has total energy 23.7V21.43Ah=159Wh, 438 while the existing vehicle has total energy 43.7V10.6Ah=157Wh. We see that the 439 total energy is almost the same for both the designs. 440

AQ1

AQ2



this figure will be printed in b/w

Fig. 8 Influence of the number of rotors on the design vector for payload equal to 1 kg. Objective functions comparison

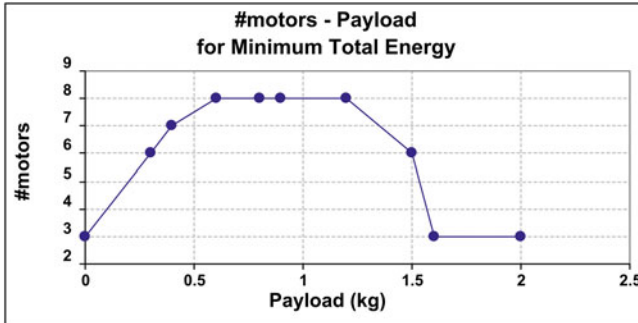
this figure will be
printed in b/w

Fig. 9 Influence of payload on the number of rotors for minimum energy

this figure will be
printed in b/w

Fig. 10 (Left) The quadrotor Walkera HM Hoten X Quadcopter. (Right) The Octocopter X88-J2

Table 1 Optimized and actual Walkera HM Hoten X Quadcopter comparison

Model	Walkera Hoten X Quadcopter	Optimization	Difference	t1.1
#Motors	4	4	0	t1.2
Payload capacity (f_w)	2	2	0	t1.3
Total flight time (min)	10	10	0	t1.4
Total mass (kg)	0.332	0.283	-0.05	t1.5
Payload (kg)	0.1	0.100	0.00	t1.6
Vehicle mass (kg)	0.269	0.237	-0.03	t1.7
Battery capacity (Ah)	1	1.611	0.61	t1.8
Battery #cells	2	1	-1	t1.9
Battery mass (kg)	0.064	0.046	-0.02	t1.10
Propeller diameter (m)	0.186	0.184	0.00	t1.11
Vehicle diameter (m)	0.500	0.510	0.01	t1.12

Conclusions

441

This work focused on the parametric design and optimization of a multi-rotor aerial vehicle (MRAV). Using simplified models of propulsion system components such as motors, propellers, electronic speed controllers (ESC), and battery, a

442

443

444

Table 2 Optimized and actual Octocopter X88-J2 comparison

Model	X88-J2 Octocopter	Optimization	Difference	
#Motors	8	8	0	t2.1
Payload capacity (f_w)	1.51	1.51	0	t2.2
Total flight time (min)	17.5	17.5	0	t2.3
Total mass (kg)	3.11	3.23	0.12	t2.4
Payload (kg)	1.13	1.13	0.00	t2.5
Vehicle mass (kg)	2	2.10	0.10	t2.6
Battery capacity (Ah)	10.6	21.43	10.83	t2.7
Battery #cells	4	2	-2	t2.8
Battery mass (kg)	1.11	1.22	0.11	t2.9
Propeller diameter (m)	0.305	0.24	-0.07	t2.10
Vehicle diameter (m)	1.205	0.91	-0.29	t2.11

total model for an MRAV was created and the whole system performance at 445 hovering and at maximum thrust was described. Additionally, based on the technical 446 specifications of commercially available batteries, motors, and ESCs, component 447 functional parameters were expressed as a function of component size, in terms of 448 an equivalent length. As a result, we were able to calculate system performance 449 as a function of a design vector which consists of each individual component 450 equivalent length. A Matlab program was developed which calculates the optimal 451 design vector using the “fmincon” function. The total energy consumption and the 452 vehicle diameter were considered as objective functions. As a result, for a given 453 payload, payload capacity, number of rotors, and flight duration, the optimal size 454 of each component that minimizes energy or MRAV size was calculated. Finally, 455 using the developed program, we were able to study the influence of the payload, 456 and of the number of rotors, on the design vector and the MRAV size. The results 457 obtained by the program were compared to existing commercial MRAVs, showing 458 that the developed methodology yields designs close to reality. In addition, this 459 methodology provides an MRAV designer with the tools to improve an existing 460 design. 461

References

462

1. F. Kendoul, Survey of advances in guidance, navigation, and control of unmanned rotorcraft systems, *Journal of Field Robotics*, Vol. 29, No 2, pp. 315–378, March/April 2012, 463
464
2. Q. Jiang, et al, Analysis and Synthesis of Mult-Rotor Aerial Vehicles, *Proceedings of the 465 ASME 2011 International Design Engineering Technical Conferences & Computers and 466 Information in Engineering Conference, IDETC/CIE 2011*, August 28–31, Washington, DC, 467 USA, DETC2011-47114, 2011. 468
3. D. Langkamp, et al, An engineering development of a novel hexrotor vehicle for 3D 469 applications, *Proceedings Micro Air Vehicles Conference 2011*, Summer edition, 2011. 470
4. N. Fernandes, Design and construction of a multi-rotor with various degrees of freedom, M.S. 471 Thesis, Technical Univ. of Lisboa, 2011. 472

5. F. Bohorquez, et al., Design, Analysis and Hover Performance of a Rotary Wing Micro Air Vehicle, *Journal of the American Helicopter Society*, Vol. 48, No 2, pp. 80–90, 2003. 473
6. A. Harrington, Optimal Propulsion System Design for a Micro Quad Rotor, M.S. Thesis, University of Maryland, 2011. 475
7. D. Lundström, K. Amadori, P. Krus, Automation of Design and Prototyping of Micro Aerial Vehicle, *AIAA-2009-629*, 47th AIAA Aerospace Sciences Meeting, Orlando, FL, USA, Jan. 2009. 477
8. S. Bouabdallah, Design and Control of Quadrotors with Application to Autonomous Flying, Ph.D. Thesis, École Polytechnique Federale de Lausanne, 2007. 480
9. J.G. Leishman, *Principles of Helicopter Aerodynamics*, Cambridge University Press, New York, 2006. 482
10. J. Brandt, and M. Selig, Propeller Performance Data at Low Reynolds Numbers, 49th AIAA Aerospace Sciences Meeting, AIAA 2011-1255. <http://www.ae.illinois.edu/m-selig/props/propDB.html>, 2011. 484
11. Walkera HM Hoten X Quadcopter - 200 size, <http://www.helifreak.com/showthread.php?t=452889>. 488
12. X88-J2 Octocopter, <http://www.wowhobbies.com/x88octocopter.aspx>. 489

AUTHOR QUERIES

- AQ1. Please check the sentence “with total energy $23.7V1Ah=7.4Wh$, while the optimized needs $13.7V1.611Ah=6Ah$ ” is ok.
- AQ2. Kindly check the sentence “Thus, the optimized vehicle has total energy $23.7V21.43Ah=159Wh$, while the existing vehicle has total energy $43.7V10.6Ah=157Wh$ ” is ok.

UNCORRECTED PROOF